ISSN 0018-151X, High Temperature, 2010, Vol. 48, No. 2, pp. 231–237. © Pleiades Publishing, Ltd., 2010.
Original Russian Text © N.N. Zubkov, A.F. Polyakov, Yu.L. Shekhter, 2010, published in Teplofizika Vysokikh Temperatur, 2010, Vol. 48, No. 2, pp. 250–256.

HEAT AND MASS TRANSFER AND PHYSICAL GASDYNAMICS

The Hydraulic Characteristics of Porous Materials for a System of Transpiration Cooling

N. N. Zubkov[a], A. F. Polyakov[b], and Yu. L. Shekhter[b]

[a] *Bauman Moscow State Technical University, Moscow, 105005 Russia*

[b] *Joint Institute for High Temperatures, Russian Academy of Sciences (IVTAN), Moscow, 125412 Russia*

Received December 26, 2008

Abstract—As a result of laboratory and numerical experiments, data on hydraulic drag and structure of flow are obtained for the first time in samples of sheet porous material prepared using the ingenious technology of two-way strain cutting. The study is aimed at developing an efficient system of transpiration cooling with tangential injection of cooling gas onto a microrough surface.

DOI: 10.1134/S0018151X10020148

INTRODUCTION

The development of a highly efficient system of transpiration cooling requires the use of materials and technologies which would provide for the stability and reproducibility of the hydraulic and thermal characteristics of envelopes in the process of manufacture and operation, as well as their "predictability" in designing. A porous mesh material (PMM) was investigated in the first stage as the sheet material for the system of transpiration cooling. Extensive thermomechanical, hydraulic, and thermal testing was performed. The major advantage of PMM consists in the orderliness and reproducibility of its structure. At the same time, the use of PMM for ensuring distributed injection and thermal protection of curvilinear surfaces involves serious (often insurmountable) difficulties. The foregoing requirements must be taken into account in developing systems of transpiration cooling of the leading edges of gas turbine blades, where high pressure gradients are realized in the external flow of high-temperature gas. The new unique technology of strain cutting makes it possible to produce a sheet porous material free of disadvantages typical of PMM.

This paper gives a brief description of the method of preparing sheet porous material by means of two-way strain cutting (SPMTSC) and of the results of investigation of its hydraulic characteristics. In particular, samples were investigated, which are provided with special tangential outlet channels intended for developing a highly efficient system of transpiration cooling of the leading edges of bodies subjected to flow. Data on hydraulic drag of SPMTSC are compared with the available data for PMM.

SHEET POROUS MATERIAL PREPARED BY MEANS OF TWO-WAY STRAIN CUTTING

Investigations of a new method of shaping based on the processes of both cutting and plastic strain [1, 2] are under way at Bauman Moscow State Technical University. The method received the name of "strain cutting". The use of this method, which has been patented in major industrially developed countries [3], results in qualitatively new characteristics of permeable porous materials.

The method of strain cutting is based on blade machining and on simultaneous strain of the undercut surface layers of the blank and the forming of close-spaced deep and narrow grooves. The plurality of layers, which were undercut by the main cutting edge and did not separate from the blank, form a surface macrorelief in the form of ribs. The width of the grooves may range from several microns to hundreds of microns, with the depth of the grooves being tens of times their width. A model of the zone of cutting is given in Fig. 1.

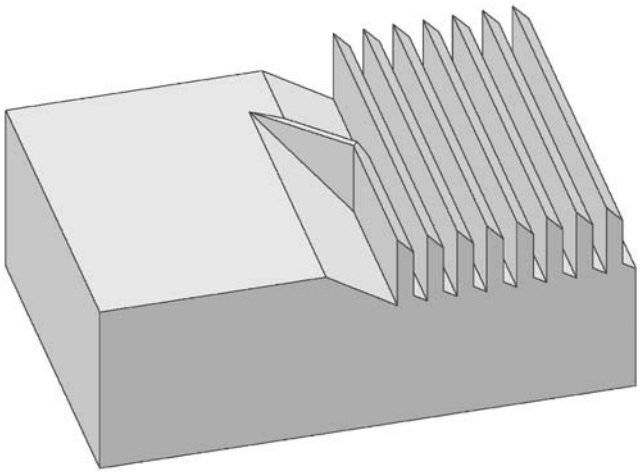

Fig. 1. A model of the zone of cutting.

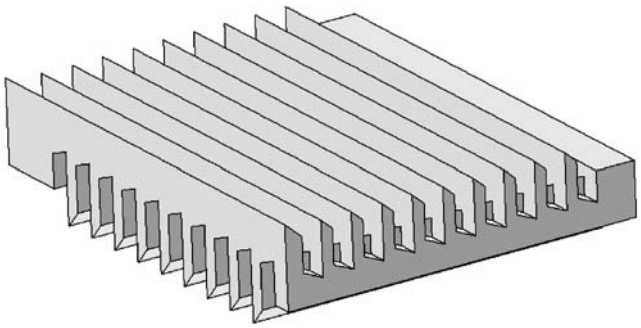

Fig. 2. A model of permeable envelope.

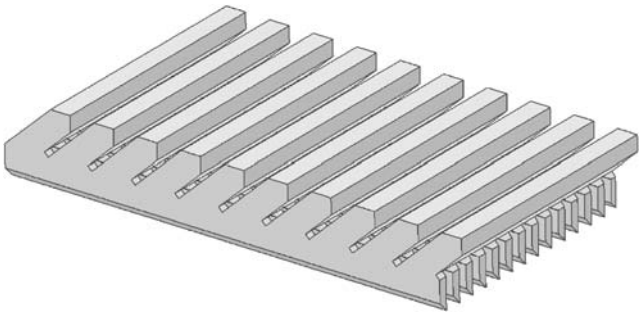

Fig. 3. A model of permeable envelope with tangential channels.

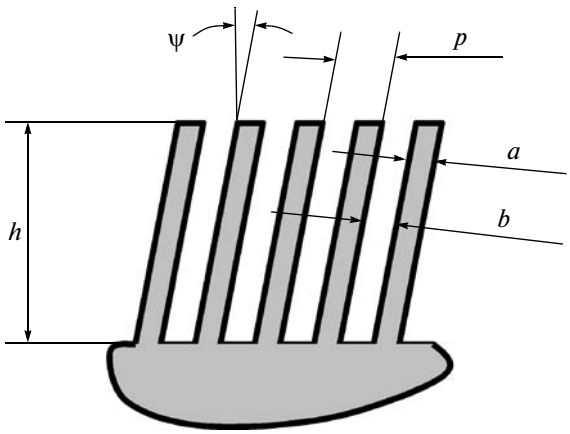

Fig. 4. Parameters of SPMTSC.

The permeable envelope for subsequent use in transpiration cooling is prepared as a result of machining of two sides of a sheet metal blank by the method of strain cutting. The permeable structure is essentially prepared by providing the ribbing on both sides of the blank in the directions normal to each other; in so doing, the depth of cutting in the machining of each side must exceed half the thickness of the sheet being processed. As a result, a permeable sheet structure is obtained with square or rectangular inside shape of openings. The cooling gas outlet on the sheet surface is slotted. A parametric model of the structure of permeable envelope is given in Fig. 2. This method makes possible the shaping of surfaces with distributed injection and specially organized microroughness, including tangential outlet channels. Such geometric parameters of surface cannot be attained using any one of the existing methods of mechanical or physicotechnical processing. The local characteristics of the resultant permeable partition over its area may be controlled by ribbing one or both sides of the sheet with variable pitch. A permeable envelope with tangential outlet channels for cooling gas may be provided by making inclined ribbing on one side of the sheet; in so doing, the ribbing on the other side of the sheet may be noninclined (Fig. 3).

In preparing permeable partitions by the method of strain cutting, the geometric parameters on which the characteristics of gas flow being injected depend are fully defined by the parameters of ribbed structures obtained on the opposite sides of the sheet blank. The parameters of ribbed structure are as follows (Fig. 4): p, the pitch of ribbing; ψ, the inclination of the ribs to the base; h, the height of ribbing; and a, the rib thickness. Important parameters further include the desired width of groove b and the surface porosity of the structure Π given by the relation $\Pi = b/(p\cos\psi)$.

A sheet blank of 03Kh17N14M3 (chrome–nickel–molybdenum) steel for preparing sample no. 1 of permeable envelope (Fig. 2) was 0.3 mm thick. The opposite sides of the sheet blank were processed identically. The ribbing is provided with the width of interrib gap of 33% of the pitch (interrib spacing plus rib width), namely, $b = 83$ μm. The pitch of ribbing is $p = 0.25$ mm. The rib height is $h = 0.3$ mm on one side and $h = 0.4$ mm on the other side. The finished sample thickness was $l = 0.6$ mm. Therefore, the total height of the openings is 0.1 mm. The surface porosity is $\Pi_{1s} = 0.33$. The bulk porosity determined both by weighing and by calculation by channel geometry is $\Pi_1 = 0.37$.

The possibility of preparing permeable partitions with inclined outlet channels (for ensuring tangential injection of cooling gas) was checked in a model material with a large margin of plasticity. The model material was provided by M1 copper (sample no. 2, Fig. 3). The initial thickness of the blank was 1.0 mm. The width of slot outlets on the sheet side with inclined ribbing was $b = 80$ μm. The pitch of ribbing was $p = 0.5$ mm and the rib slope $\psi = 43^0$. The height of inclined ribs was $h = 0.58$ mm. The ribbing on the other side of the sheet was made with vertical arrangement of the ribs and the interrib gap width of 0.365 mm. The pitch of ribbing was $p = 0.7$ mm. The height of straight ribs was $h = 1.22$ mm. The permeable sample thickness was $l = 1.6$ mm. The height of the overall volume of openings was 0.2 mm. The bulk

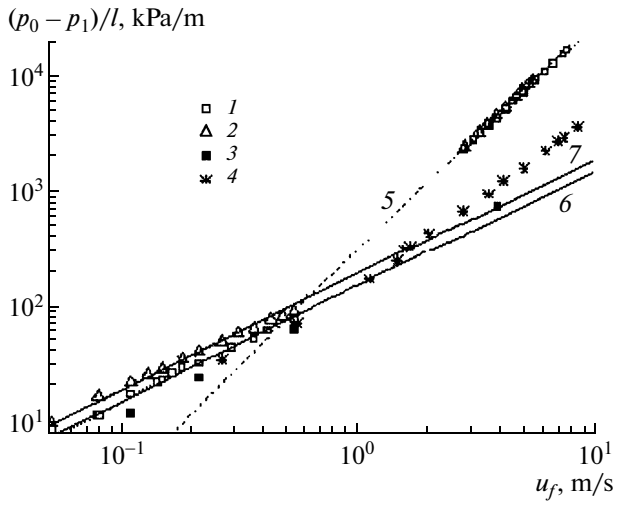

Fig. 5. The specific hydraulic drag of porous sheet samples. Experimental data for SPMTSC: (*1*) sample no. 1 with straight channels on both sides, (*2*) sample no. 2 with inclined channels on one side and straight channels on the other side, (*3*) calculation for sample no. 1, (*4*) experimental data for PMM [7]. Approximation lines: (*5*) connection of experimental points *1*, *2* in turbulent region, (*6*) connection of experimental points *1* in laminar region, (*7*) connection of experimental points *2* in laminar region.

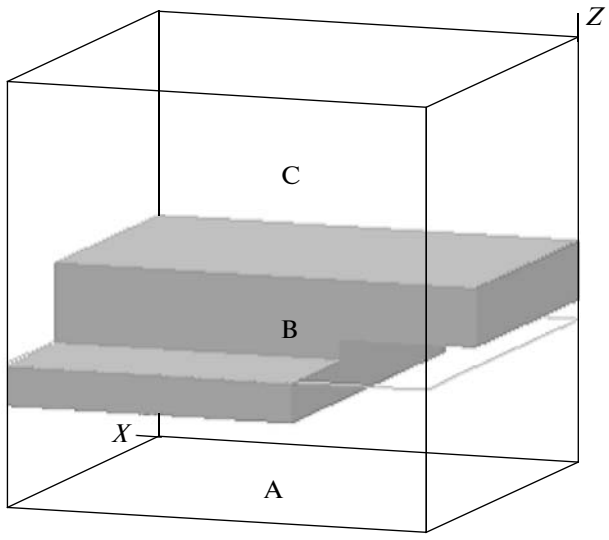

Fig. 6. Computational volume (proportions are not observed).

porosity determined both by weighing and by calculation by channel geometry was $\Pi_2 = 0.5$.

HYDRAULIC CHARACTERISTICS OF SPMTSC

Experimental Investigation of Hydraulic Drag

The hydraulic drag of SPMTSC was determined using its flat samples 40 mm in diameter, which were placed at the exit section of Witoszynski nozzle. The dependence $\Delta p = f(u_f)$ was measured, which was used to find the hydraulic drag coefficients.

All measurements were performed with air under atmospheric conditions. The investigated range of mass velocity of air was 0.05–8 kg/(m^{2}s). Special attention was given to the region of low velocities of injection which provided, under conditions of laminar flow in a porous layer, for unseparated outflow of cooling gas into the boundary layer of hot gas in a system of transpiration cooling.

Figure 5 gives, in coordinates of filtration rate (velocity away from the porous envelope) u_f–$\Delta p/l$ (drop per unit thickness of porous layer), all of the results of measurements for two described samples of SPMTSC (points *1* and *2*). The conventional linear dependence of hydraulic drag on the velocity of moving medium is observed at low velocities of gas flow in the laminar mode. Two continuous straight lines *6* and *7*, which pass at $u_f < 0.6$ m/s through the experimental points *1* and *2*, respectively, are described by the dependences $\Delta p/l = c_{1,2}u_f$, where $c_1 = 150$ and $c_2 = 190$. As usual, the square law is realized in the inertial region with separated flows. In so doing, the following feature is observed. While in the linear region the specific drag for sample no. 2 with inclined channels (points *2*) is somewhat higher than that for sample no. 1, the data for both samples in the square region almost coincide (line *5*). It is possible that this difference in the case of laminar flow is associated with the somewhat greater length of channels in the sample with inclined channels.

Numerical Simulation of the Flow Structure and Drag in SPMTSC Microchannels

Along with laboratory experiment, numerical experiment was performed involving analysis of the flow structure and drag in SPMTSC models analogous with sample no. 1. The three-dimensional steady isothermal flow of gas in SPMTSC microchannels was calculated using the ANES computer codes developed by V.I. Artemov at the Moscow Institute of Power Engineering (MEI) [4, 5]. Leontiev and Polyakov [6] used the ANES computer codes in the case of slotted porous layer for performing numerical experiment involving the flow structure and heat transfer in the porous layer. In this idealized formulation, the solution of two-dimensional problem was obtained. However, SPMTSC is a real product with strictly preassigned geometry of microchannels, which enables one to perform numerical calculation of flow and heat transfer for each concrete sample. Naturally, this calls for the solution of three-dimensional problem.

Figure 6 gives the x, *y*, *z* three-dimensional computational domain. The air is fed uniformly to the supply

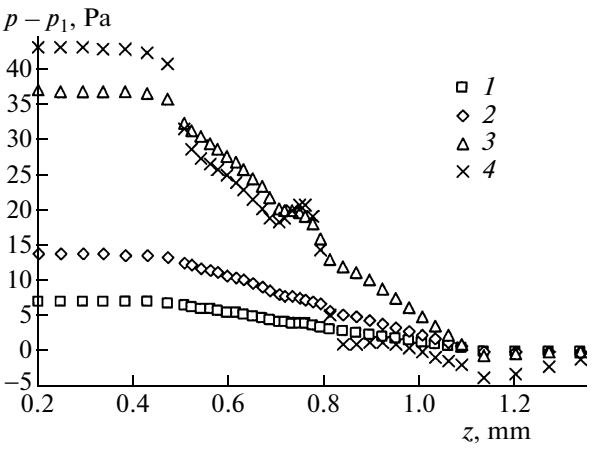

Fig. 7. The distribution of pressure along coordinate z on the line passing at the center of "square" through opening: (*1*) $\mathrm{Re}_e = 3.3$, (*2*) 6.5, (*3*) 16.6, (*4*) 118 (the values of $(p - p_1)/10$ are plotted for this mode).

zone A and moves along the z axis. The zone B accommodates a quarter of an SPMTSC cell—half pitch $(a + b)$ on both coordinates x, y, namely, $(b_x/2 + a_x/2)$, $(a_y/2 + b_y/2)$ (see Figs. 2 and 4). In the zone C, the gas flows out into a free volume.

The conditions of symmetry are assigned on the side boundaries of the typical element of SPMTSC, i.e., zero values of derivatives of all three components of velocity.

Figure 7 gives the distributions of pressure along the line passing at the center of through opening $x = 0$, $y = (a_y + b_y)/2$ from the beginning to the end of calculated length $(0 \le z \le L_0 + L + L_1)$. The values of Reynolds number $\mathrm{Re}_e = u_f d_e/(\Pi\nu)$ are determined by the equivalent diameter $d_e = 4V/S = 0.17$ mm, which is very close to the equivalent diameter of slotted channels at the inlet and outlet of the porous layer $d_{e0} = d_{e1} = 2b = 0.16$ mm. Here, V is the total volume of the channels, S is the surface being wetted, and the subscripts 0 and 1 relate to the inlet into porous layer and outlet from this layer, respectively. The upstream region (zone A) is $L_0 = 0.5$ mm, the porous layer thickness is $L = 0.6$ mm (zone B), and the region of gas removal is $L_1 = 1$ mm (zone C). In Fig. 7, the upstream and removal regions are shortened. The pressure varies almost linearly over the entire thickness of the porous layer under conditions of laminar unseparated flow, where $\mathrm{Re}_e < 20$ (points *1*–*3*), except for minor deviation in the region of intersection of grooves along coordinate y on the inlet side of the porous sheet (shown by straight lines in Fig. 6) and along coordinate x on the outlet side; this deviation is 0.1 mm (0.7 mm $\le z \le$ 0.8 mm). In the case of Reynolds number values of $\mathrm{Re}_e > 100$ (points *4*), where rather intensive separated flows are formed, the pressure variation is nonmonotonic. A significant pressure drop is observed in the vicinity of outlet of gas from the porous layer even compared to pressure away from the outlet p_1 taken to be the value of reading. The points *4* demonstrate the qualitative pattern of hydrodynamics for relatively high values of Reynolds number; however, the employed procedure of numerical experiment does not enable one to closely follow different-scale vortex flows in this case, in spite of agreement with iteration count for the mode under consideration. This situation naturally affects the integral value of pressure difference over the porous layer thickness. Indicative of this is the calculated value of specific pressure difference under these conditions given in Fig. 5 (point *3* at $u_f = 3.9$ m/s), which is significantly (in fact, by an order of magnitude) lower than the experimentally obtained value. At the same time, at $\mathrm{Re}_e < 20$, the calculated points of $(p_0 - p_1)/L$ are close to the experimental points. The somewhat higher experimentally obtained values are apparently associated with the edge effect along the perimeter of attachment of experimental sample to the nozzle set. This effect was ignored in the calculations, because a symmetric cell in the inner part of the sample was considered. Moreover, it is our objective to develop an efficient system of transpiration cooling which permits no separation of gas flow on the surface subjected to flow. Therefore, the working modes in this case will be those with $\mathrm{Re}_e < 20$.

Figure 8 gives the distributions of velocity component u_z in two planes passing through the planes of symmetry of the outlet channel, namely, x–z plane at $y = (a_y/2 + b_y/2)$(Fig. 8a), and of the inlet channel, namely, y–z plane at $x = 0$ (Fig. 8b). The dark strips with thicker mesh pass in channels in porous layer. We will start considering the plane passing through the inlet channel (Fig. 8b). The uniform value of velocity $u_0 \equiv u_f = 0.215$ m/s is assigned at the beginning of the plane under consideration, as in the case of the entire surface with $z = 0$. The velocity significantly increases at the channel inlet ($z = 0.5$ mm), because the surface of inflow of gas is smaller than the total area, namely, the average value of the velocity of gas flow into the porous layer is $\overline{u}_z\big|_{z=L_0} = u_0(a+b)^2/(b(a+b)) = 0.215 \times 0.25/0.08 = 0.67$ m/s. In Fig. 8b at $z = L_0 = 0.5$ mm, the value $u_z \cong 1$ m/s is uniform in the plane of symmetry of the inlet channel, and the distribution of u_z across the inlet channel on coordinate x for this value of z is given in Fig. 8a. On the channel wall ($x = b_x/2 = b/2 = 0.04$ mm), we have $u_z = 0$. The minimal thickness of the sheet on the inlet side (lower part in Fig. 6) $h_0 = 0.2$ mm is shown in Fig. 8a by the side with zero value of velocity $u_z = 0$ along coordinate z ($0.5 \le z \le 0.7$ mm, $0.04 \le x \le 0.125$ mm). Note that the parabolic velocity profile with $u_z^{\max}\big|_{z=L_0} = 1.5\overline{u}_z\big|_{z=L_0}$ is already formed

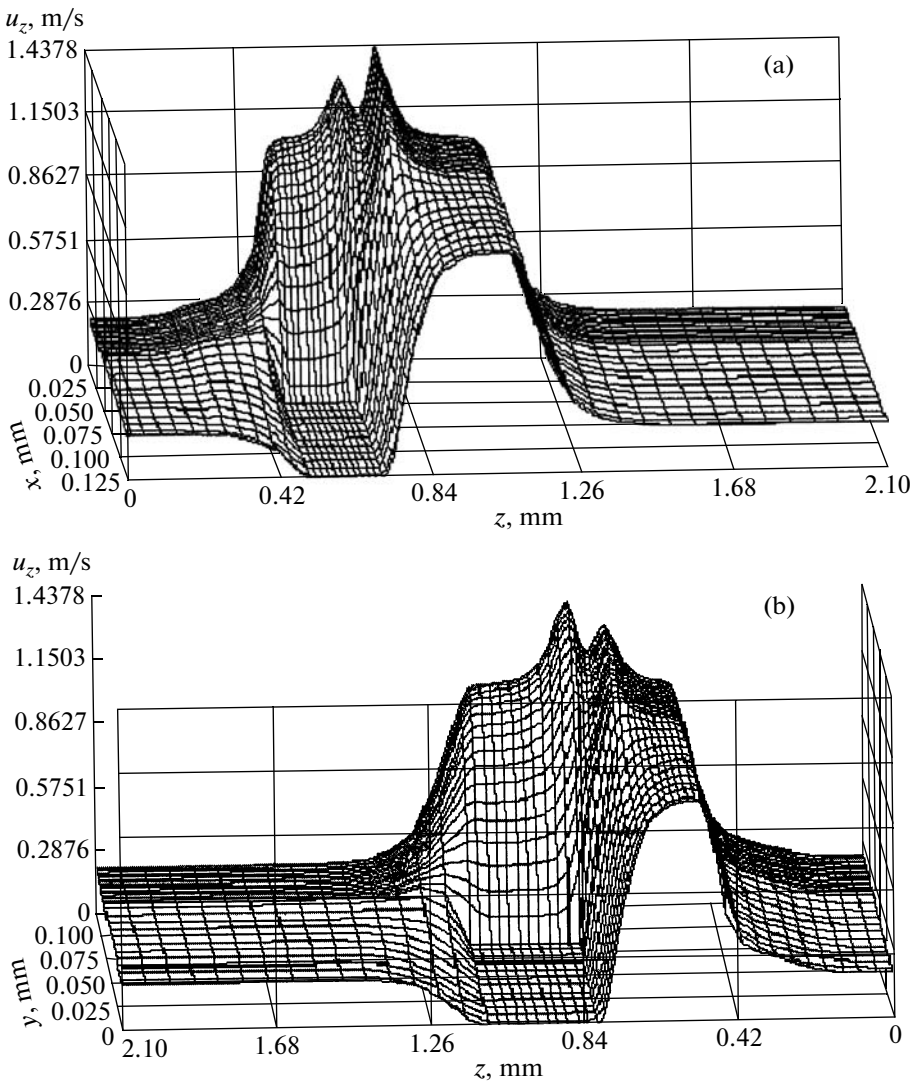

Fig. 8. The distributions of longitudinal component of velocity at $\mathrm{Re}_e = 6.5$ in planes passing on the axis of through channel: (a) plane of symmetry of the outlet channel ($y = a/2 + b/2$), (b) plane of symmetry of the inlet channel ($x = 0$).

at the inlet to plane channel; this profile is typical of steady laminar flow in plane channels [7].

The extreme lines in both graphs of Fig. 8 with two peaks characterize the distribution of longitudinal component of velocity along the line of intersection of planes of symmetry of channels, i.e., the central line of through opening ($x = 0, y = a_y/2 + b_y/2$). We will trace the variation of velocity by moving along this line from the previously considered parabolic distribution of u_z with respect to x in the cross section $z = L_0 = 0.5$mm (Fig. 8a). During the motion from $z = 0.5$ mm to $z = 0.7$ mm, shown by continuous line in Fig. 6, the distribution of u_z is deformed owing to the increase in the maximum, the value of which reaches $u_z^{\max} \cong 1.25$ m/s. This occurs as a result of delivery of gas along the y axis from under the upper shelf of porous plate, as one can judge from Fig. 8b. After leaving the lower shelf at a distance of 0.1 mm to the approach to the upper shelf, i.e., from 0.7 to 0.8 mm, an overall free space exists of intersection of the lower (along y) and upper (along x) channels. In this region, the maximum of u_z somewhat decreases at the beginning of opening of the channels and then abruptly increases to $u_z^{\max} \cong 1.44$ m/s owing to the reduction of free surface at the inlet to the upper shelf zone. The upper shelf 0.3 mm thick, which is shown in Fig. 8b by the rectangle with $u_z = 0$, is in the range $0.8 \le z \le 1.1$mm. At the outlet from the upper channel, the velocity which is uniform along the channel has almost the same parabolic distribution across the channel (Fig. 8b, $z = 1.1$ mm) as that at the inlet to the porous layer (Fig. 8a, $z = 0.5$ mm).

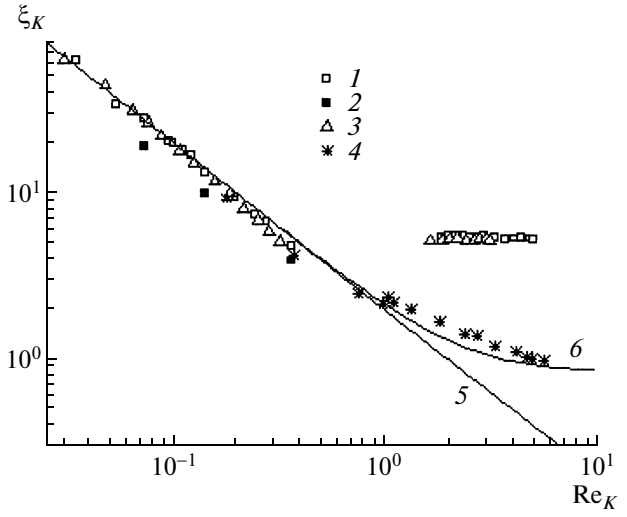

Fig. 9. The hydraulic drag coefficient as a function of Reynolds number: (*1*) SPMTSC sample no. 1 with straight channels on both sides; (*2*) results of numerical solution for sample no. 1; (*3*) SPMTSC sample no. 2 with inclined channels on one side and straight channels on the other side; (*4*) experimental data for PMM [7]; (*5*) $\xi_K = 2/\mathrm{Re}_K$, Eq. (1); (*6*) calculation by the predicted dependence suggested in [9] for the parameters corresponding to experimental points *4*.

A positive factor is the fact that, in spite of the presence of a bounded through opening, the velocity before the outlet from the porous layer is equalized along the channel. The velocity of gas exit from the porous layer is equalized throughout the layer surface at a distance of approximately 0.25 mm from this surface (Figs. 8a and 8b). When SPMTSC with tangential outlet openings is employed, the scale model of which is provided by the experimentally investigated sample no. 2, one can safely speak about a still smoother exit of gas onto the surface subjected to flow. However, special experiments in the investigation of the structure of wall flow are required for obtaining a more detailed pattern of gas flow on a surface with tangential openings.

ANALYSIS OF DATA ON THE DRAG OF ENVELOPE POROUS MATERIALS

The hydraulic characteristics of sheet PMM were investigated in [8–10]. The hydraulic drag of PMM in a wide range of values of Reynolds number was generalized in [10] using the permeability coefficient K [m^2]. The conventional relations for hydraulic drag using $\sqrt{K}$ as the characteristic linear scale will take the form

$$\Delta p/L = (p_0 - p_1)/L = (1/K)\mu u_0 + B\rho u_0^2 = (\xi_K/\sqrt{K})(\rho u_0^2/2), \quad (1)$$

$$\xi_K = (2/\mathrm{Re}_K) + 2B\sqrt{K}, \quad (2)$$

where $\mathrm{Re}_K = u_0\sqrt{K}/\nu$. The equality in Eq. (1) is the generalized Darcy equation, where $(1/K)$ is the coefficient of viscosity and B is the inertial coefficient; the second equality is written using the overall coefficient of hydraulic drag ξ.

The permeability coefficients for the tested SPMTSC samples nos. 1 and 2, which were determined by the experimental data given in Fig. 5, are $K_1 = 1.2\times10^{-10}$ m^2 and $K_2 = 0.94\times10^{-10}$ m^2, respectively.

For PMM sample no. 014 of square mesh with percent reduction in the process of hot rolling being $\varepsilon = 0.4$, the average pore size is 0.09 mm, with the porosity $\Pi_{net} \cong 0.5$ and permeability coefficient $K_{net} = 1.2\times10^{-10}$ m^2 [8, 10]. All of the foregoing parameters for the selected PMM sample and for SPMTSC sample no. 1 tested by us are close to one another.

Along with the data for SPMTSC, Fig. 5 gives experimental data on specific pressure difference in the selected PMM sample (points *4*). In the region of laminar flow, points *4* coincide with the data for SPMTSC sample no. 1; however, in the case of PMM, the laminar flow is retained at somewhat higher velocities of gas flow. The special features of variation of hydraulic drag of SPMTSC and PMM are observed more clearly in Fig. 9 in coordinates of Eq. (2). The relaxation to constant values of coefficient of hydraulic drag in the turbulent region occurs in SPMTSC much before it does in PMM; in so doing, the values of this coefficient in the former case are much higher.

CONCLUSIONS

Data were obtained for the first time on hydraulic drag and structure of gas flow in sheet porous material prepared using the unique technology of two-way strain cutting.

The specific hydraulic drag of sheet porous material prepared by means of two-way strain cutting coincides with that of sheet porous mesh material for the same pore sizes in the mode of laminar flow of gas. However, the laminar flow in the former case is realized at lower values of Reynolds number. In the case of turbulent flow, the hydraulic drag coefficients for both materials are self-similar relative to the gas flow rate; however, the values of these coefficients are much higher for SPMTSC than for PMM.

ACKNOWLEDGMENTS

This study was supported by the Russian Foundation for Basic Research (grant nos. 07-08-12136-ofi, 06-08-00146-a, 09-08-00151-a).

REFERENCES

1. Zubkov, N.N., *Tekhnol. Mashinostr.*, 2001, no. 1, p. 19.
2. Zubkov, N.N. and Sleptsov, A.D., *Izv. Vyssh. Uchebn. Zaved. Mashinostr.*, 2007, no. 3, p. 56.
3. Zoubkov, N.N. and Ovtchinnikov, A.I., US Patent 5 775 187, 1998.
4. Artemov, V.I., Makarov, M.E., Murov, A.G. et al., Numerical Simulation of the Processes of Heat and Mass Transfer in the ANES System, in *Trudy MMF-92* (Proceedings of MMF-92), Minsk: Izd. ITMO (Lykov Inst. of Heat and Mass Transfer), 1992.
5. Artemov, V.I., Yan'kov, G.G., Karpov, V.E., and Makarov, M.E., *Teploenergetika*, 2000, no. 7, p. 52.
6. Leontiev, A.I. and Polyakov, A.F., *Teplofiz. Vys. Temp.*, 2008, vol. 46, no. 6, p. 881 (*High Temp.* (Engl. transl.), vol. 46, no. 6, p. 811).
7. Petukhov, B.S., *Teploobmen i soprotivlenie pri laminarnom techenii zhidkosti v trubakh* (Heat Transfer and Drag under Conditions of Laminar Flow of Liquid in Pipes), Moscow: Energiya, 1967.
8. Zeigarnik, Yu.A., Polyakov, A.F., Sukhoruchenko, S.Yu., and Shekhter, Yu.L., *Teplofiz. Vys. Temp.*, 1996, vol. 34, no. 6, p. 924 (*High Temp.* (Engl. transl.), vol. 34, no. 6, p. 910).
9. Polyakov, A.F., Sukhoruchenko, S.Yu., and Shekhter, Yu.L., *Teplofiz. Vys. Temp.*, 2000, vol. 38, no. 2, p. 284 (*High Temp.* (Engl. transl.), vol. 38, no. 2, p. 264).
10. Polyakov, A.F., Strat'ev, V.K., Sukhoruchenko, S.Yu. et al., *Izv. Ross. Akad. Nauk Energ.*, 2000, no. 3, p. 118.